

ESTABLISHMENT OF CONSTITUTIVE MODEL AND DYNAMIC PARAMETER ANALYSIS OF RUBBER CONVEYOR BELT

HONGYUE CHEN, SIYUAN LIU

School of Mechanical Engineering, Liaoning Technical University, Fuzin, China

Corresponding author Siyuan Liu, e-mail: 1392451428@qq.com

A rubber conveyor belt is an essential piece of equipment in coal mine transportation. Its current motion and performance are directly affected by dynamic parameters. In this paper, a constitutive model has been established to study a rubber conveyor belt in order to analyze its dynamic characteristics. The covered rubber was considered as a classical solid model. The wire rope core was used as a Kelvin model, and a generalized constitutive mathematical model was established. Using Matlab, comparison of the fitting curve and the experimental curve was carried out to ensure reliability in an appropriate way. Meanwhile, the influence of different factors on dynamic parameters of rubber conveyor belts was also discussed by controlling the loading frequency and amplitude as well as external temperature. Finally, the experiment with the fitting curve was compared and verified, and the research results can provide a reference for this engineering field.

Keywords: rubber conveyor belt, wire rope core, kinetic parameters, fitting curve, mathematical model

1. Introduction

As the most economical and efficient large-scale bulk material conveying system globally, the belt conveyor system is widely used in all walks of life. One of the most commonly used systems is the rubber belt conveyor. However, with the increasing demand for conveying volume and continuous improvement of conveying efficiency, large-capacity, long-distance and high-speed conveyors have become the direction of development. However, this puts forward higher requirements for rubber conveyor belts (Yang *et al.*, 2010) due to strong nonlinearity of rubber material properties and the influence of temperature, excitation frequency and excitation amplitude. Based on the Fourier series, we propose a two-dimensional and three-dimensional boundary element formula for a compressible viscoelastic layer with any thickness, which reveals the viscoelastic effect of rubber materials due to their own asymmetry (Zéhil and Gavin, 2014). Therefore, it is essential for the constitutive model of the rubber conveyor belt and the analysis of its dynamic parameters.

As a kind of viscoelastic material, the constitutive model of a rubber conveyor belt belongs to the scope of viscoelastic mechanics. In the theory of viscoelastic mechanics, the stress-strain-time relation of a viscoelastic material can be divided into differential and integral types. The stress-relaxation behavior of rubber composites was studied using the extension index of the Collauche equation and the Maxwell-Weichert model (Maria *et al.*, 2014). In recent years, the viscoelastic constitutive relation has been significantly developed by introducing fractional derivatives. The fractional Maxwell model, the fractional Kelvin model, and the three-force superposition model were developed by Sjöberg and Kari (2002). The indentation area was measured by strain gauges, and the variation law of stress when a specific point on the rubber conveyor belt was rolled over the idler was analyzed (Jonkers, 1999). According to Spaans (2001), the energy consumption method deduced a calculation formula for indentation resistance. Lodewijks (2013) carried out a viscoelasticity test for rubber with different compositions by a dynamic mechanical analyzer

DMA, which provided a valuable reference for studying the influence of characteristics of the covering layer on the indentation resistance. Rudolphi and Reicks (2006) selected the generalized Maxwell model to characterize viscoelastic properties of the covering layer, and to fit the previous viscoelastic test results. They deduced a formula for calculating the indentation resistance.

Wang *et al.* (2007) proposed a visco-hyperelasticity model after superelasticity and viscoelasticity to test rubber materials in a wide strain range. Zhu *et al.* (2015) used a nonlinear and fractional derivative viscoelasticity (FDV) model to discuss the relationship between stiffness and damping and the excitation frequency and displacement amplitude. It was concluded that the dynamic stiffness and damping of the guide rail pad increased with the excitation frequency and decreased with an increase of the displacement amplitude. Zhang and Xia (2011) explored the energy conversion in the operation process of the belt conveyor and improved the operation efficiency through an optimization method. Qiu and Chai (2011) applied viscoelastic and Winkler basic assumptions to discuss the effects of viscoelastic characteristics, transport rate and speed on the energy loss of the transport system. Gil-Negrete *et al.* (2006) used a finite element (FE) code to predict dynamic stiffness of the filled rubber separator, evaluated dynamic stiffness of the actual liner under working conditions and used the equal effect variable amplitude value estimation, and the prediction results were reliable. Chen *et al.* (2015) deduced parameters of a conveyor belt expressed by a three-parameter constitutive model, and Liu *et al.* (2010) carried out finite element verification and optimization of viscoelasticity of the covering rubber. Cho *et al.* (2013) interpolated a temperature dependence of the rubber loss modulus by using a reasonable 4-parameter fitting method, and solved the loss of the temperature-nonlinear hysteresis and temperature distribution by using an interleaved iterative calculation scheme. Through numerical experiments, the prediction results were compared with the experimental results to verify the effectiveness of the prediction method. Hao *et al.* (2008) constructed a generalized recovery model for rubber. Tong *et al.* (2020) proposed a new nonlinear viscoelastic constitutive model to describe mechanical behavior of rubber composites. Behnke and Kaliske (2015) proposed a numerical framework for effective thermodynamic analysis of a full three-dimensional rubber tire structure (axially symmetric geometry) in steady state motion, discussed parameter identification in detail focusing on the rolling resistance and surface temperature distribution. Gholipour *et al.* (2020) first developed and solved the coupled continuous viscoelastic model based on Timoshenko's nonlocal strain gradient theory. Nguyen *et al.* (2020) proposed a structural damage diagnosis method based on the change of mechanical parameters of rubber. Chen *et al.* (2020) established and simulated a rigid-flexible coupling dynamic model of belt conveyor based on theoretical analysis.

In previous studies, many mechanical models and simulation algorithms describing dynamic characteristics of rubber conveyor belts have been obtained. It is concluded that the classical solid model and Kelvin model can well describe mechanical characteristics of rubber conveyor belts with steel wire core under a stress state, and the constitutive model of a steel wire rubber conveyor belt can better describe dynamic characteristics of operation. The ST1600 type rubber conveyor belt is regarded as the research object. The belt consists of the upper rubber cover, lower rubber cover, core rubber and a steel wire rope embedded in the core rubber, as shown in Fig. 1. This paper further improves the constitutive model by applying the previous theory and samples used in the experiment based on previous studies. Through mathematical fitting of two variables of the frequency and amplitude, this paper discusses the influence of the amplitude and frequency on the elastic modulus and damping of the rubber conveyor belt. At the same time, the frequency and amplitude are controlled by an experimental method, and the simulation results are verified to ensure reliability of the results. The dynamic characteristics of steel wire rope rubber conveyor belts are analyzed by combining the theory and experiment to analyze stress characteristics of rubber conveyor belts in industrial transportation in coal mines. Since the steel wire rope embeds the inner core rubber, the bolt body is composed of rubber. The

rubber material has some viscoelastic characteristics. It can be seen that the rubber conveyor belt has dual physical and mechanical properties. If the load changes during the operation, its elastic modulus and damping coefficient will also change. It can be seen that the self-recovery force of the rubber conveyor belt is a nonlinear relationship. Hence, the research on deformation resistance of the rubber conveyor belt has a practical application value.

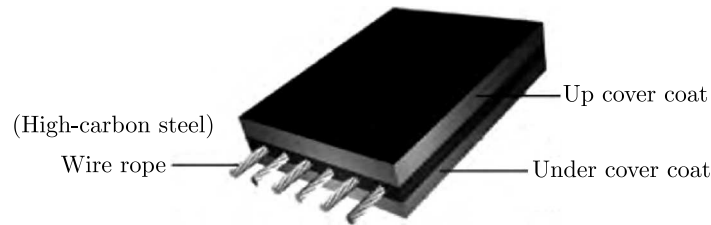


Fig. 1. Model of a rubber conveyor belt

2. Theoretical basis

In this paper, the examined object is a steel cord rubber conveyor belt. It is often used in coal mine transportation, and the typical failure mode is steel cord degumming. To study dynamic characteristics of rubber conveyor belts, it is necessary to study a mathematical model. The whole working process of the rubber conveyor belt can be understood as a steel wire core bearing a tensile force and rubber bearing the load of gravity.

2.1. Fourier series

The Fourier series is widely used in algebra, combinatorics, signal processing, probability theory, statistics, cryptography, acoustics, optics and other fields. The formula is shown in (2.1)

$$\begin{aligned} f(t) &= \frac{a_0}{2} + a_1 \cos(\omega t) + b_1 \sin(\omega t) + a_2 \cos(2\omega t) + b_2 \sin(2\omega t) + \dots \\ &= \frac{a_0}{2} + \sum_{n=1}^{\infty} [a_n \cos(n\omega t) + b_n \sin(n\omega t)] \end{aligned} \quad (2.1)$$

where

$$a_n = \frac{2}{T} \int_{t_0}^{t_0+T} f(t) \cos(n\omega t) dt \quad b_n = \frac{2}{T} \int_{t_0}^{t_0+T} f(t) \sin(n\omega t) dt \quad (2.2)$$

The Fourier series describes the periodic function $f(t)$ as a constant coefficient a_0 and a sum of sin and cos functions of 1 times ω , sin and cos functions of 2 times ω , and sin and cos functions of n times ω . Each term has different coefficients a_n and b_n . These coefficients need to be calculated by integration. For convenience, the integration interval is generally set to the width of one cycle T . This paper studies the influence of the loading frequency and amplitude on rubber conveyor belts. The loading frequency and amplitude changes have periodic characteristics and can be treated as sinusoidal functions. Using the Fourier series to process such information enables comparison and process of data more intuitively, reduction of errors caused by repeated data processing, and improvement of data processing efficiency and reliability.

2.2. Kelvin model

The Kelvin model is an ideal spring parallel with an ideal damper with no transient elastic effect on stress or strain. As $t \rightarrow \infty$ (t – time), the creep of the Kelvin model tends to be an asymptote, which is characteristic for viscoelastic solids in stable creep. The Kelvin model is often used in conjunction with the Maxwell model, which is composed of the two units connected in series. The two units are mostly ideal dampers and ideal springs. When an external force acts on this model, the external force in the spring and the dashpot is the same. Under specific stress, the material can deform infinitely, which is characteristic for viscous fluids. The transient response of the Maxwell model is characteristic for an elastic body, while the time effect is characteristic for a viscous fluid. When applied to the model, the total stress is shared by the spring and damper, and the total strain is the sum of the two.

The application of the Kelvin model is essential for establishing the constitutive model. The establishment of the constitutive model of the steel cord rubber conveyor belt is based on the Kelvin model. It provides prerequisites for formulating a mathematical model and simulation analysis in this paper.

3. Constitutive model of the conveyor belt

In order to make the calculation straightforward, a simplified model of the rubber conveyor belt is established to analyze the stress-strain relationship. Different materials have different constitutive relations under different deformation conditions, also known as different constitutive models. In essence, it is a physical relationship. The equations established are called physical equations which comprehensively reflect the macroscopic mechanical properties of structures or materials. In a broad sense, it is a sweeping curve of a generalized force-deformation or a strength-deformation law. Various materials, components or structures may have many different reactions in various stress stages. However, if the generalized force-deformation curve is drawn, all phenomena of different reactions will have similar and corresponding geometric characteristic points on the curves. Accordingly, the application of the constitutive model, which is consistent in macroscopic scale, will be of great use in theoretical research and engineering practice.

In an ideal state, each steel wire rope inside the conveyor belt is evenly embedded, the force is the same and uniform during operation, the performance parameters of each steel wire rope are the same, and the calculation and analysis process are relatively simple. Therefore, we assume that the rubber conveyor belt is currently in an ideal working state. Under stable working conditions, the shear deformation between the steel wire rope and rubber is small and can be ignored. The shear force between the steel wire core and rubber can also be ignored, the covering rubber is regarded as a classical solid model and the core is considered a Kelvin material.

In Fig. 2, $E_{f1}E_{fn}$ denotes the elastic modulus of each wire rope [MPa]. It represents the stress required to produce unit deformation per unit area and characterizes the ability of the material to resist elastic deformation. The larger the value, the greater the energy to resist elastic deformation. $\eta_{f1}\eta_{fn}$ stands for the damping coefficient of each wire rope; n is the total number of wire ropes, E_{m1} , E_{m2} are the elastic moduli of the rubber matrix [MPa]. The larger the damping coefficient, the greater the damping force generated by the same velocity. η_m is the damping coefficient of the rubber matrix [MPa·s]. In this paper, the Kelvin model is used to describe behavior characteristics of the steel wire which is regarded as a spring and damping element. $E_{f1}E_{fn}$ represents the elastic modulus of each steel wire and describes the ability of it to resist deformation. The larger the elastic modulus the smaller deformation and the stronger the steel wire under the same force. Since the material and geometric parameters of the wire used in the conveyor belt are exactly the same, the elastic modulus of each wire is the same,

that is, $E_{f1} = E_{f2} = \dots = E_{fn}$. A single steel wire is loaded by the sinusoidal load, see Eq. (4.1) in Section 4.1, and the curve is fitted by the Fourier series. The parameters are shown in equations (4.2)-(4.5) to complete the calculation of elastic modulus E of the steel wire.

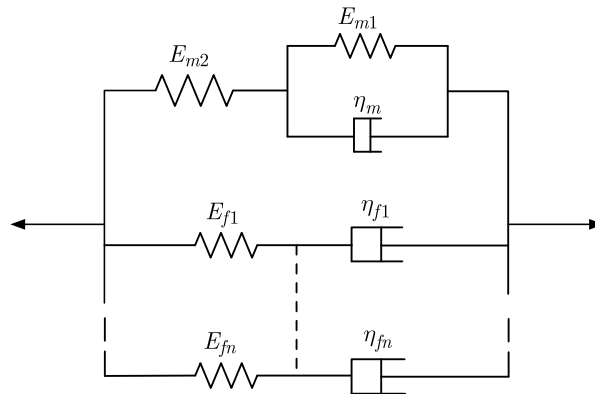


Fig. 2. Constitutive model of the rubber conveyor belt

The rubber conveyor belt and the steel wire core of the dual steel cable belong to elastic materials, rubber belongs to hyperelastic materials. The steel wire core is a skeleton, and the rubber is used as the cladding with viscoelastic properties. In this paper, mechanical characteristics of overburden rubber are regarded as in a classical solid model, and mechanical characteristics of the wire core are regarded as in the Kelvin model. A generalized constitutive model is established, which can not only reflect the relaxation and creep characteristics of the conveyor belt, but also express the transient response during loading. The load during operation can be regarded as a sinusoidal change, so the loading displacement has sinusoidal character. A smooth operation process of the steel wire reinforced rubber conveyor belt can be regarded as uniform linear motion. The rubber conveyor belt maintains a balanced state along the axial direction of the steel wire core. In the actual working process of belt, although there is tension along the axial direction, the deformation is small, which does not affect the motion state of the rubber conveyor belt, so the classical solid model and Kelvin model are used as a theoretical basis to establish the equation of equilibrium of the constitutive model

$$\begin{aligned} \sigma &= n\sigma_f v_f + \sigma_m(1 - v_f) & \sigma_f &= E_f \varepsilon_f + \eta_f \dot{\varepsilon}_f & \varepsilon &= \varepsilon_{m1} + \varepsilon_{m2} \\ \sigma_m &= E_{m1} \varepsilon_{m1} = E_{m2} \varepsilon_{m2} + \eta_m \dot{\varepsilon}_{m1} & \varepsilon &= \varepsilon_f \end{aligned} \quad (3.1)$$

In the formula, v_f is the volume fraction of each wire, σ is the stress of the belt [MPa], σ_f is the stress of each wire [MPa], σ_m is the stress matrix of rubber [MPa], ε is the strain of the steel wire core, which indicates deformation of the conveyor belt (dimensionless). The strain matrix of the rubber is regarded as ε_{m1} , ε_{m2} and indicates deformation of the stressed rubber (dimensionless). The strain of each wire is regarded as ε_f which indicates deformation of the wire under stress (dimensionless).

The generalized constitutive mathematical model of the rubber conveyor belt is obtained by combining and simplifying the equation of the system (3.1)

$$\sigma = (E_f \varepsilon + \eta_f \dot{\varepsilon}) n v_f + (-p_1 \dot{\sigma} + q_0 \varepsilon + q_1 \dot{\varepsilon})(1 - v_f) \quad (3.2)$$

where

$$p_1 = \frac{\eta_m}{E_{m1} + E_{m2}} \quad q_0 = \frac{E_{m1} E_{m2}}{E_{m1} + E_{m2}} \quad q_1 = \frac{\eta_m E_{m1}}{E_{m1} + E_{m2}}$$

$\dot{\sigma}_m$ is the first derivative of σ_m with respect to time t and the $\dot{\varepsilon}$ is the first derivative of ε .

The external load dynamic strain of the conveyor belt is

$$\varepsilon = A \sin(\omega t) + \varepsilon_0 \quad (3.3)$$

where ε_0 is the initial strain, A – strain amplitude [mm].

Substituting (3.3) into (3.2), one gets

$$\begin{aligned} \sigma(t) = & [E_f \varepsilon_0 + E_f A \sin \omega t + \eta_f A \omega \cos(\omega t)] n v_f \\ & + \left[q_0 \varepsilon_0 + \frac{A(q_1 \omega^2 p_1 + q_0)}{1 + \omega^2 p_1^2} \sin(\omega t) + \frac{A(q_1 - q_0 p_1) \omega}{1 + \omega^2 p_1^2} \cos(\omega t) \right] (1 - v_f) \end{aligned} \quad (3.4)$$

The length of the conveyor belt is denoted by L , and the cross-sectional area by S . At the same time, it is assumed that the displacement of the loaded conveyor belt by angular excitation is

$$x = M \sin(\omega t) + x_0 \quad (3.5)$$

where x_0 – initial loading displacement [mm], M – load displacement amplitude [mm], ω – loading angular frequency [rad/s].

The following equation can express strain of the belt

$$\varepsilon = \frac{x}{L} \quad (3.6)$$

According to formula (3.6), the initial strain is $\varepsilon_0 = x_0/L$.

The following equation can express the strain amplitude

$$A = \frac{M}{L} \quad (3.7)$$

Substituting the strain amplitude and initial strain into equation (3.4), equation (3.4) becomes

$$\begin{aligned} \sigma(t) = & \frac{x_0}{L} [n E_f v_f + q_0 (1 - v_f)] + \frac{M}{L} \sin(\omega t) \left[n E_f v_f + \frac{q_1 \omega^2 p_1 + q_0}{1 + \omega^2 p_1^2} (1 - v_f) \right] \\ & + \omega \frac{M}{L} \cos(\omega t) \left[n \eta_f v_f + \frac{q_1 - q_0 p_1}{1 + \omega^2 p_1^2} (1 - v_f) \right] \end{aligned} \quad (3.8)$$

Under the displacement excitation, the force of the conveyor belt will change dynamically. It can be expressed as

$$F = \sigma(t) S \quad (3.9)$$

where F is the force of the conveyor belt under the displacement excitation in [N], S is the cross-section area of the conveyor belt in [mm²].

Substituting equation (3.8) into (3.9), we get

$$\begin{aligned} F = & \frac{x_0}{L} [n E_f v_f + q_0 (1 - v_f)] + \frac{M}{L} S \sin(\omega t) \left[n E_f v_f + \frac{q_1 \omega^2 p_1 + q_0}{1 + \omega^2 p_1^2} (1 - v_f) \right] \\ & + \omega \frac{M}{L} S \cos(\omega t) \left[n \eta_f v_f + \frac{q_1 - q_0 p_1}{1 + \omega^2 p_1^2} (1 - v_f) \right] \end{aligned} \quad (3.10)$$

4. Parameter prediction and validation

4.1. Experiment preparation

The general steel cord rubber conveyor belt ST1600 that meets GB/T 9770-2013 is selected as the research object in this paper. As shown in Fig. 3, the length of the selected sample is 1100 mm, width is 75 mm, and thickness of the upper and lower covering glue is 6 mm. The thickness of the core rubber is 5 mm, there are six steel wire ropes inside, and the diameter of the steel wire core is 5 mm. Although the rubber conveyor belt is subjected to weight of the materials, friction and tension during operation, the action of these forces makes the rubber conveyor belt displace. Therefore, the displacement represents the action of various forces acting on the rubber conveyor belt. The electronic universal tensile testing machine was used to load the sample in this experiment. A sinusoidal displacement loading was used as the initial loading during this experiment. The frequency f was 0.1 Hz, the amplitude M was 1.4 mm, and the initial displacement x_0 was 1.9 mm. The loading function is given by the formula

$$x = 1.4 \sin(0.2\pi t) + 1.9 \text{ mm} \quad (4.1)$$

Since the vibration frequency is about 0.1 Hz under a heavy load in the actual working process, 0.1 Hz is selected as the loading frequency. There is tension in the conveyor belt installation process and an initial position is generated. In this scheme, the initial position is 1.9 mm. In this paper, the maximum width of the conveyor belt is 1.5 mm, and such limiting cases rarely occur, so the loading amplitude of 1.4 mm is selected for the study.

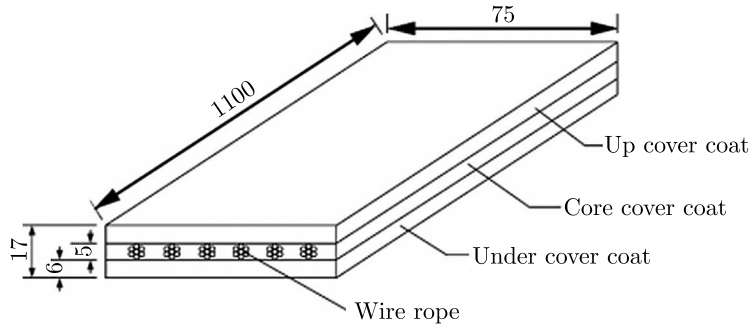


Fig. 3. Schematic diagram of the sample structure

4.2. Experimental verification

According to the relevant knowledge of material mechanics and structural mechanics, the external load equation of the wire rope is

$$F_f(t) = \frac{x_0 E_f S_f}{L} + \frac{M S_f E_f}{L} \sin(\omega t) + \frac{\omega M S_f \eta_f}{L} \cos(\omega t) \quad (4.2)$$

where F_f is the force of the wire rope under the displacement excitation in [N]; S_f is the section area of the wire rope in [mm²].

A first-order Fourier series can fit the force-displacement curve of a viscoelastic material, and the fitting function is as follows

$$F(t) = a_0 + a_1 \cos(\omega t) + b_1 \sin(\omega t) \quad (4.3)$$

According to formula (4.2) and (4.3), it can be known that

$$a_0 = \frac{x_0 E_f S_f}{L} \quad a_1 = \frac{\omega M S_f \eta_f}{L} \quad b_1 = \frac{M S_f E_f}{L} \quad (4.4)$$

According to formula (4.4), we can get

$$E_f = \frac{a_0 L}{x_0 S_f} \quad \eta_f = \frac{a_1 L}{\omega S_f M} \quad (4.5)$$

The displacement-force curve of a single wire rope is fitted by the Matlab cftool tool, and a_0 , a_1 and b_1 can be obtained. The elastic modulus and damping coefficient of the wire rope model are calculated by using a_0 , a_1 and b_1 . In this paper, GB/T 9770-2013 ordinary steel wire core rubber conveyor belt ST1600 is selected, and the steel wire used in the core is the same as in GB/T 12753-2020 conveyor belt. By calculation, $E_f = 9735.3$ MPa, $\eta_f = 683.9$ MP·s.

The external load equation of the rubber conveyor belt base is given as

$$F_m = \frac{x_0 S_m q_0}{L} + \frac{M S_m (q_1 \omega^2 p_1 + q_0)}{L(1 + \omega^2 p_1^2)} \sin(\omega t) + \frac{\omega M S_m (q_1 \omega^2 p_1 + q_0)}{L(1 + \omega^2 p_1^2)} \cos(\omega t) \quad (4.6)$$

where F_m is the force of the rubber substrate under displacement excitation in [N]; S_m is the section area of the rubber substrate in [mm²].

From equations (4.6) and (4.4), it can be found that

$$a_0 = \frac{x_0 S_m q_0}{L} \quad a_1 = \frac{\omega M S_m (q_1 \omega^2 p_1 + q_0)}{L(1 + \omega^2 p_1^2)} \quad b_1 = \frac{M S_m (q_1 \omega^2 p_1 + q_0)}{L(1 + \omega^2 p_1^2)} \quad (4.7)$$

Deduced from equations (4.6) and (4.7)

$$E_{m1} = \frac{L(a_1^2 x_0 + b_1^2 x_0 + a_0 b_1 M)}{S_m M(x_0 b_1 - a_0 M)} \quad E_{m2} = \frac{a_0 L(a_1^2 x_0 + b_1^2 x_0 - a_0 b_1 M)}{S_m(a_1^2 x_0 + b_1^2 x_0^2 - 2a_0 b_1 x_0 M + a_0^2 M^2)}$$

$$\eta_m = \frac{a_0 L(a_1^2 x_0 + b_1^2 x_0 - a_0 b_1 M)^2}{a_1 S_m(a_1^2 x_0 + b_1^2 x_0^2 - 2a_0 b_1 x_0 M + a_0^2 M^2)} \quad (4.8)$$

The rubber matrix displacement-force curve is fitted with the Matlab cftool tool from which a_0 , a_1 and b_1 can be obtained, and the elastic modulus and damping coefficient of the wire rope model is calculated using a_0 , a_1 and b_1 .

It has been calculated that $E_{m1} = 684.6$ MPa, $E_{m2} = 2059.7$ MPa, $\eta_m = 5487.4$ MPa·s.

In order to verify correctness of the theoretical model of the rubber conveyor belt, a test has been conducted in a universal tensile test machine and a digital display temperature control box. The experimental equipment and materials are shown in Fig. 4. In order to avoid the test data being affected by temperature, first, the sample is placed at a room temperature of 25°C for 12 hours. With the experimental data unaffected by temperature, the specimen is then fixed in the testing machine with a load applied to one end and a fixed clamp at the other end. The strain amplitude is controlled between 0.5 mm-3.6 mm, the frequency is 0.1 Hz, the loading changes according to the sine law, the experimental data is exported, and the exported data is put into Matlab for comparison with the theoretical curve, as shown in Fig. 5, the reliability is analyzed.

The digital display temperature control box ensures that the temperature of the experimental process is constant and ensures that the experimental results are not affected by external temperature. In the experiment, the upper and lower fixtures of the universal tensile test machine is 1000 mm. An experiment with the sinusoidal displacement loading of the conveyor belt is performed, and then the reliability of the current mechanical model is analyzed according to the experimental data. The size of the conveyor belt used for the loading test is: width 75 mm, thickness 17 mm, wire core diameter 5 mm, upper and lower cover layer rubber thickness 6 mm, upper and lower fixture interval 1000 mm, fixture clamping part 50 mm, the selected conveyor



Fig. 4. Experimental equipment and materials

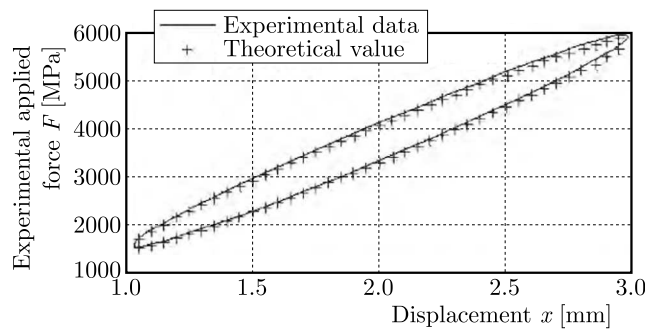


Fig. 5. Theoretical curve and the actual curve

belt specimen length 1100 mm. The calculation process of the characteristic parameters of the conveyor belt is shown in Eqs. (4.2)-(4.8). The section area of the wire is S_f , and that of the rubber substrate is S_m .

According to Fig. 5, it can be seen that the experimental and simulation results have a reasonable degree of agreement. The coefficient of coincidence of the two curves is 0.96, which can meet the accuracy requirements of the actual working conditions.

The curve error map is generated by Matlab, as shown in Fig. 6.

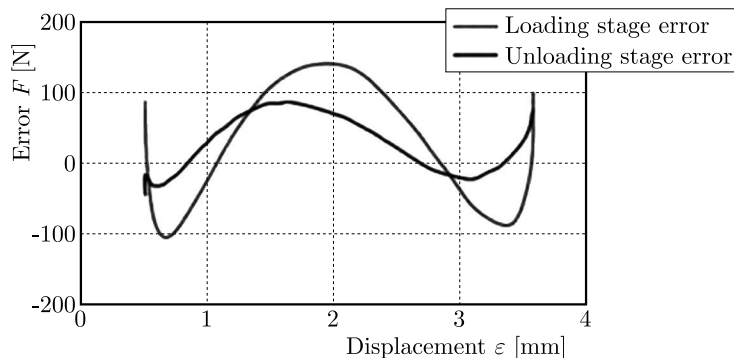


Fig. 6. Curve error diagram

It can be seen from the curve error diagram that the maximum error is 148 N, and the operation is not significantly affected. Therefore, it is advisable to explore mechanical parameters of the rubber conveyor belt described by the constitutive model and applicable in the coal transportation process.

5. Analysis of parameter changes

5.1. Amplitude and frequency changes

Since viscoelasticity is possessed by the material of the rubber conveyor belt itself, there are differences in the damping coefficient η_m and elastic moduli E_{m1} , E_{m2} of the rubber conveyor belt under different loads. It is of practical research value to explore the influence of the load on these parameters. Investigated is the influence of the load on the characteristics of rubber conveyor belt through loading amplitude and loading frequency. When the rubber conveyor belt is working normally, the elongation per unit length under the maximum load condition is 3.6 mm, and the maximum elongation in normal working conditions is between 2.0-3.6 mm. The conveyor belt has dead weight, and the elongation per unit length under no load condition is about 0.5 mm. Therefore, the minimum displacement is selected as 0.5 mm, and the maximum displacements of loading are 2.0 mm, 2.5 mm, 2.7 mm, 3.0 mm and 3.5 mm. The identification results are shown in Table 1. It can be seen that the damping coefficient η_m first decreases and then increases, and the elastic modulus E_{m1} increases slightly but rapidly. It can be seen that as the loading displacement increases, the rigidity of the conveyor belt increases as well.

According to the data in Table 1, the relationship between the loading amplitude M and the damping coefficient η_m , elastic moduli E_{m1} , E_{m2} is fitted to determine the relationship between different amplitudes and the damping coefficient η_m and the elastic moduli E_{m1} , E_{m2} .

Table 1. Parameters of the conveyor belt model for changing load amplitude

Serial number	Frequency f [Hz]	Amplitude M [mm]	Initial value x_0 [mm]	Damping coefficient η_m [MPa·s]	Elastic modulus E_{m1} [MPa]	Elastic modulus E_{m2} [MPa]
1	0.10	0.75	1.25	7349.40	1812.27	16161.88
2	0.10	1.00	1.50	5829.19	1811.64	16333.88
3	0.10	1.10	1.60	4646.56	1804.29	16949.18
4	0.10	1.25	1.75	5726.50	1789.69	19332.34
5	0.10	1.50	2.00	6189.91	1721.71	29190.33

Using Matlab software to perform quadratic polynomial fitting, the fitting results are as follows

$$\begin{aligned}
 \eta_m(M) &= (4.78M^2 - 12.67M + 13.92) \cdot 10^3 \\
 E_{m1}(M) &= (-0.04M^2 - 0.14M + 1.98) \cdot 10^3 \\
 E_{m2}(M) &= (9.32M^2 - 6.22M + 14.01) \cdot 10^3
 \end{aligned} \tag{5.1}$$

The certainty coefficients between the fitted curve and the original data are 0.81, 0.88 and 0.94, respectively, and the certainty coefficients are relatively low. Therefore, verification of prediction accuracy is required.

The values of $f = 0.1$ Hz, amplitude $M = 1.45$ mm, initial displacement $x_0 = 1.95$ mm are substituted into formula (5.1) for verification and comparison of the prediction results with the identification results, as shown in Table 2.

It can be seen from Table 2 that the relative error between the identification results of the damping coefficient η_m and the prediction results is the largest. However, it is only 3.76%, which can still meet the actual needs of the project. It can be seen that the needs of predicting the belt operation by Eqs. (5.1) is satisfied.

Chen *et al.* (2017) used viscoelastic dynamics theory and the Fourier series fitting method to derive and establish the parameter identification equation of the standard solid model of a rubber conveyor belt. For a constant frequency of 0.10 Hz, the amplitudes are, respectively, 0.75 mm,

Table 2. Comparison of prediction and identification parameters

	Damping coefficient η_m [MPa·s]	Elastic modulus E_{m1} [MPa]	Elastic modulus E_{m2} [MPa]
Identification result	5816.84	1701.47	24285.60
Forecast result	5598.40	1692.90	24586.00
Relative error [%]	3.76	0.50	1.24

1.00 mm, 1.25 mm, 1.50 mm, 1.75 mm, 2.00 mm. The damping coefficient η_m is 7340.49 MPa·s, 5892.09 MPa·s, 5750.26 MPa·s, 6135.89 MPa·s, 7068.83 MPa·s, 7629.77 MPa·s. The elastic modulus E_{m1} is 1812.64 MPa, 1817.27 MPa, 1730.69 MPa, 1621.71 MPa, 1609.19 MPa, 1571.28 MPa and the elastic modulus of E_{m2} is 16160.88 MPa, 16336.15 MPa, 18322.34 MPa, 29190.33 MPa, 32789.09 MPa, 37425.32 MPa. The law of parameter change shows that the damping coefficient η_m decreases first and then increases, and the elastic moduli E_{m1} and E_{m2} both increase, but the growth rate of E_{m1} is far smaller than that of E_{m2} , which is consistent with the change law of the experimental results. The experimental method, experimental data and experimental conclusions are reliable.

Table 3. Conveyor belt model parameters for changing frequency

Serial number	Frequency f [Hz]	Amplitude M [mm]	Initial value x_0 [mm]	Damping coefficient η_m [MPa·s]	Elastic modulus E_{m1} [MPa]	Elastic modulus E_{m2} [MPa]
1	0.02	1.25	1.75	6326.46	1777.00	45124.94
2	0.05	1.25	1.75	6067.00	1758.03	38278.99
3	0.08	1.25	1.75	5810.73	1749.01	23465.56
4	0.10	1.25	1.75	5726.50	1740.69	19332.34
5	0.12	1.25	1.75	5385.27	1721.71	16856.33

The loading frequency expresses a typical change in the load during operation of the conveyor belt. Therefore, the influence of the loading frequency on the conveyor belt needs to be discussed. Here, the loading amplitude is kept constant, and the loading frequency is set to 0.02 Hz, 0.05 Hz, 0.08 Hz and 0.10 Hz. The conveyor belt is loaded at 0.12 Hz, and the identification results are shown in Table 3. It can be concluded that with an increase of the loading frequency, the damping coefficient η_m and elastic moduli E_{m1} , E_{m2} both decrease, and the change rate of E_{m2} is faster and more apparent.

According to the data in Table 3, the relationship between the loading amplitude f and damping coefficient η_m as well as elastic moduli E_{m1} , E_{m2} is fitted to determine the relationship between different amplitudes and the damping coefficient η_m and the elastic moduli E_{m1} , E_{m2}

$$\begin{aligned}
 \eta_m(f) &= (-8.66f^2 - 7.34f + 6.47) \cdot 10^3 \\
 E_{m1}(f) &= (-1.9f^2 - 0.25f + 1.68) \cdot 10^3 \\
 E_{m2}(f) &= (1183f^2 - 477.4f + 56.54) \cdot 10^3
 \end{aligned} \tag{5.2}$$

In equation (5.2), the fitting coefficients between the three fitting curves and the original data are 0.98, 0.99 and 0.96, respectively. The three curves have a good fitting relationship with the original data and have a high degree of approximation. The needs for forecasting operation of the belt are met.

5.2. Temperature change

Although coal mining is mostly underground, it changes with working conditions and external environmental temperature. The wire rope rubber conveyor belt is used for underground transportation, and the operating temperature is usually not lower than 0°C and not higher than 40°C. Therefore, a loading experiment is conducted every 10°C interval between 0°C and 40°C, and the loading frequency $f = 0.1$ Hz, amplitude $M = 1.25$ mm and initial displacement $x_0 = 1.75$ mm are selected to discuss the influence of temperature change on the conveyor belt parameters.

This experiment was conducted with a universal stretching test machine and incubator as shown in Fig. 4. First, the incubator temperature was set to 0°C, after 10 minutes to ensure the accurate temperature, then adjusted to 10°C, kept constant for 10 minutes, and then raised up to 20°C, 30°C and 40°C. The parameter identification results are shown in Table 4. It can be seen that the damping coefficient η_m and the elastic moduli E_{m1} and E_{m2} both decrease with an increase of temperature. The elastic modulus E_{m1} changes once linearly, E_{m2} quadratically. E_{m1} is less affected by temperature than E_{m2} . The damping coefficient η_m is greatly affected by temperature after it exceeds 20°C. Its change is less affected by temperature below 20°C, and the amplitude is small. Combined with the change of the conveyor belt damping coefficient η_m and the elastic moduli E_{m1} and E_{m2} for changing amplitude and frequency, it is known that although the temperature affects the dynamic parameters of the conveyor belt, its influence is smaller than the effect of amplitude and frequency.

Table 4. Conveyor belt parameters for changing temperature

Serial number	Temperature T [°C]	Frequency f [Hz]	Amplitude M [mm]	Initial value x_0 [mm]	Damping coefficient η_m [MPa·s]	Elastic modulus E_{m1} [MPa]	Elastic modulus E_{m2} [MPa]
1	0	0.10	1.25	1.75	5728.97	1743.97	19339.94
2	10	0.10	1.25	1.75	5727.68	1741.89	19336.83
3	20	0.10	1.25	1.75	5727.57	1740.84	19333.57
4	30	0.10	1.25	1.75	5724.48	1740.66	19330.41
5	40	0.10	1.25	1.75	5712.55	1740.62	19327.25

According to the data in Table 4, the relationship between the temperature T and damping coefficient η_m , elastic moduli E_{m1} and E_{m2} is fitted to true relationship between these parameters

$$\begin{aligned} \eta_m(T) &= -0.0009T^3 + 0.03692T^2 - 0.449T + 5729 \\ E_{m1}(T) &= 0.0048T^2 - 0.254T + 1744 \quad E_{m2}(T) = -0.3189T + 19340 \end{aligned} \quad (5.3)$$

The equation (5.9), the fitting coefficient between the three fitting curves and the original data is 0.98, 0.94 and 0.91, respectively. The three curves have a good fitting relationship with the original data with a high approximation, which fulfills the needs for predicting the operation of the belt property.

6. Conclusions

- The classical solid model and the Kelvin model are used as the theoretical basis for establishing a generalized constitutive dynamical model of a rubber conveyor belt. Displacement and external load curves are obtained by Matlab and Fourier parameter identification and experiments, and the theoretical values are compared with the experimental ones to verify reliability of the method.

- The law of change of the dynamic parameters of the rubber conveyor belt is discussed by controlling the frequency and amplitude of the loading process. When the loading amplitude is kept constant and its frequency increases, the damping coefficient η_m and elastic moduli E_{m1} , E_{m2} both decrease, and changes of E_{m2} are more significant. When the loading frequency is kept constant and the loading amplitude increases, the damping coefficient η_m first decreases and then increases, and the elasticity moduli E_{m1} , E_{m2} both increase, but the increase and growth rate of E_{m1} are much smaller than these of E_{m2} . Next, the influence of temperature changes on the kinetic parameters of the rubber conveyor belt is discussed. Keeping the amplitude and loading frequency unchanged, the damping coefficient η_m and the elastic moduli E_{m1} and E_{m2} both decrease with an increase of temperature. The elastic modulus E_{m1} changes linearly, E_{m2} in a quadratic way, E_{m1} is less affected by temperature than E_{m2} . The damping coefficient η_m is greatly affected by temperature after it exceeds 20°C, and the change is smaller below 20°C, but the amplitude stays small.
- By establishing a mathematical model to analyze the variation law of dynamic parameters of the rubber conveyor belt, vibration and impacts in the actual transportation process of underground industrial production in the coal mine are mainly characterized by the frequency and amplitude of load. This paper discusses the influence of these factors on damping coefficient and elastic modulus. In long-distance transportation of the belt, the load is mainly borne in the steel wire rope. There will appear degumming between the steel wire rope and rubber. When the elastic modulus of rubber and damping coefficient of steel wire are lower, the stiffness of the conveyor belt is worse diminished, and the belt is more prone to deformation, degumming, and its service life is reduced. Therefore, it is necessary to select the most reasonable working frequency and amplitude by comparing and fitting the analytical results with experiments and verifying the reliability of fitting analysis to provide guidance for underground industrial coal mining.

References

1. BEHNKE R., KALISKE M., 2015, Thermo-mechanically coupled investigation of steady state rolling tires by numerical simulation and experiment, *International Journal of Non-Linear Mechanics*, **68**, 101-131
2. CHEN H.Y., HU X.B., ZHU H.D., *et al.*, 2020, Analysis of internal stress distribution characteristics of conveyor belt, *Machine Design*, **37**, 4, 55-60
3. CHEN H.Y., WANG X., ZHONG S., *et al.*, 2015, Hysteresis characteristic analysis of rubber conveyor belt and parameter prediction of restoring force model (in Chinese), *Journal of China Coal Society*, **12**, 40, 2995-3001
4. CHEN H.Y., ZHANG K., LI E.D., 2017, Parameter identification and variation rule analysis of rubber conveyor belt, *Journal of Vibration and Shock*, **14**, 234-238
5. CHO J.R., LEE H.W., JEONG W.B., JEONG K.M., KIM K.W., 2013, Numerical estimation of rolling resistance and temperature distribution of 3-D periodic patterned tire, *International Journal of Solids and Structures*, **50**, 86-96
6. GHOLIPOUR A., GHAYESH M.H., HUSSAIN S., 2020, A continuum viscoelastic model of Timoshenko NSGT nanobeams, *Engineering with Computers*, **38**, 1, 631-646
7. GIL-NEGRETE N., VIÑOLAS J., KARI L., 2006, A simplified methodology to predict the dynamic stiffness of carbon-black filled rubber isolators using a finite element code, *Journal of Sound and Vibration*, **296**, 757-776
8. HAO H.R., BAI H.B., HOU J.F., 2008, Identification of generalized restoration force model for metal-rubber, *Vibration and Shock*, **27**, 11, 105-110

9. JONKERS C.O., 1999, The indentation rolling resistance of belt conveyors: A theoretical approach, *Fördern und Heben*, **30**, 4, 384-391
10. LIU W.W., WENG X.Q., ZHU S.J., *et al.*, 2010, Research on the optimal inversion method for determining the parameters of the rubber viscoelasticity model, *Vibration and Shock*, **29**, 8, 185-190
11. LODewIJKS G., 2013, Determination of rolling resistance of belt conveyors using rubber data: Fact or fiction, *Bulk Solids Handling*, **23**, 6, 384-391
12. MARIA H.J., LYCZKO N., NZIHOu A., KURUVILLA J., CHERIAN M., SABU T., 2014, Stress relaxation behavior of organically modified montmorillonite filled natural rubber/nitrile rubber nanocomposites, *Applied Clay Science, Chinese Society of Mechanics*, **87**, 120-128
13. NGUYEN T.D., NGUYEN T.Q., NHAT T.N., NGUYEN-XUAN H., NGO N.K., 2020, A novel approach based on viscoelastic parameters for bridge health monitoring. A case study of Saigon bridge in Ho Chi Minh City – Vietnam, *Mechanical Systems and Signal Processing*, **141**, 106728
14. QIU X.J., CHAI C., 2011, Estimation of energy loss in conveyor systems due to idler indentation, *Journal of Energy Engineering*, **137**, 36-43
15. RUDOLPHI T.J., REICKS A.V., 2006, Viscoelastic indentation and resistance to motion of conveyor belts using a generalized Maxwell model of the backing material, *Rubber Chemistry and Technology*, **79**, 2, 307-319
16. SJÖBERG M., KARI L., 2002, Nonlinear behavior of a rubber isolator system using fractional derivatives, *Vehicle System Dynamics*, **37**, 3, 217-236
17. SPAANS C., 2001, The calculation of main resistance of belt conveyor, *Bulk Solids Handling*, **11**, 4, 809-825
18. TONG X., XU J., DOGHRI I., EL GHEZAL M.I., KRAIRI A., CHEN X., 2020, A nonlinear viscoelastic constitutive model for cyclically loaded solid composite propellant, *International Journal of Solids and Structures*, **198**, 4, 126-135
19. WANG R., LI S.Q., SONG S.Y., 2007, Research on basic modeling of vibration isolation rubber, *Vibration and Shock*, **26**, 1, 77-80
20. YANG C.H., MAO J., LI C.L., 2010, Research on indentation resistance of conveyor belt (in Chinese), *Journal of China Coal Society*, **35**, 1, 149-454
21. ZÉHIL G.-P., GAVIN H.P., 2014, Two and three-dimensional boundary element formulations of compressible isotropic, transversely isotropic and orthotropic viscoelastic layers of arbitrary thickness, applied to the rolling resistance of rigid cylinders and spheres, *European Journal of Mechanics A/Solids*, **44**, 175-187
22. ZHANG S.R., XIA X.H., 2011, Modeling and energy efficiency optimization of belt conveyors, *Applied Energy*, **88**, 3061-3071
23. ZHU S.Y., CAI C.B., SPANOS P.D., 2015, A nonlinear and fractional derivative viscoelastic model for rail pads in the dynamic analysis of coupled vehicle-slab track systems, *Journal of Sound and Vibration*, **335**, 304-320